

# PCCP

Accepted Manuscript



This is an *Accepted Manuscript*, which has been through the Royal Society of Chemistry peer review process and has been accepted for publication.

*Accepted Manuscripts* are published online shortly after acceptance, before technical editing, formatting and proof reading. Using this free service, authors can make their results available to the community, in citable form, before we publish the edited article. We will replace this *Accepted Manuscript* with the edited and formatted *Advance Article* as soon as it is available.

You can find more information about *Accepted Manuscripts* in the [Information for Authors](#).

Please note that technical editing may introduce minor changes to the text and/or graphics, which may alter content. The journal's standard [Terms & Conditions](#) and the [Ethical guidelines](#) still apply. In no event shall the Royal Society of Chemistry be held responsible for any errors or omissions in this *Accepted Manuscript* or any consequences arising from the use of any information it contains.



## Journal Name

## ARTICLE

## Potentiostatic current and galvanostatic potential oscillations during electrodeposition of cadmium

D. A. López-Sauri, L. Veleva\* and G. Pérez-Ángel

Received 00th January 20xx,  
Accepted 00th January 20xx

DOI: 10.1039/x0xx00000x

www.rsc.org/

Cathodic current and potential oscillations were observed during electrodeposition of cadmium from a cyanide electrolyte on a vertical platinum electrode, in potentiostatic and galvanostatic experiments. Electrochemical impedance spectroscopy experiments revealed a region of negative real impedance in a range of non-zero frequencies, in the second descending branch with positive slope of the N-Shape current-potential curve. This kind of dynamical behaviour is characteristics of the HN-NDR oscillators (oscillators with N-Shape current-potential curve and Hidden Negative Differential Resistance). The oscillations could be mainly attributed to the changes on the real active cathodic area, due to the adsorption of hydrogen molecules and their detachment from the surface. The instabilities of the electrochemical processes were characterized by time series, Fast Fourier Transforms and 2-D phase portraits showing quasi-periodic oscillations.

### Introduction

The phenomenon of spontaneous potential or current oscillations in electrochemical processes can be dated back to 1828.<sup>1</sup> The majority of electrochemical systems, for which oscillations and other interesting dynamics have been reported, involve the anodic dissolutions of various metals<sup>2-13</sup> or oxidations of molecules.<sup>14-17</sup> Only a few papers report on oscillations during electrodeposition processes and most of them are focused on galvanostatic potential oscillations.<sup>18-21</sup> Potentiostatic current oscillations have been found during electrodeposition of Cu<sup>22-23</sup> and Cu-Sn alloys from electrolyte solutions containing surfactants.<sup>24</sup> In fact, there are probably more examples of oscillating systems in electrochemistry than in any other branch of chemistry.<sup>25-28</sup>

The theoretical behaviour and classification strategies for oscillating electrochemical processes are described in several papers by Koper *et al.*,<sup>29-39</sup> which are based on impedance spectroscopy and the kinetic nature of negative faradaic impedance. The electrochemical oscillations were classified depending on whether the steady-state current-voltage exhibits (i) a negative slope with a negative impedance, or (ii) a positive slope with a "hidden" negative impedance. Even a negative impedance is not apparently indispensable for the onset of the oscillations.<sup>35</sup> The distinction of the four principal oscillator categories refers to the mechanistic role of the

double layer potential in the presence of at least one autocatalytic variable, that is, either a chemical species or an electrical quantity.<sup>38-39</sup>

-Class I is strictly potentiostatic oscillators, where the potential is non essential, while both the autocatalysis and the slow species are purely chemical.

-Class II has S-shaped voltammetric curves, where the potential is the essential slow variable with the autocatalysis still chemical.

-Class III and IV, where the potential is autocatalytic, with a chemical species forming the slow, negative feedback. Despite the common features both categories exhibit distinct dynamical behaviour. Class III exhibits a negative real impedance in combination with a region of negative slope in their steady-state current-voltage curve, and it is referred to as "NDR oscillators", because of the indispensable presence of the negative differential resistance. Class IV has a "hidden" negative impedance, coupling with a positive slope in the steady-state current-voltage curve, and they are called "H-NDR oscillators".

Even if these principal four classes represent a complete classification scheme, it is not excluded that the introduction of further subcategories may become appropriate in the future.

The model based on the concept of additional current carrier originated an interesting discussion in the literature on the role of convection in the onset of electrochemical instabilities. For example, iodate reduction with N-shape current-potential relationship, due to a Frumkin repulsive effect and hydrogen evolution, as an additional current carrier (current given rise to a reaction involving charge transfer), are emphasized in the NDR-based model, without considering the convection mass transfer.<sup>37</sup> An alternative explanation also involves hydrogen

\*Departamento de Física Aplicada, Centro de Investigación y de Estudios Avanzados (CINVESTAV-IPN), Carr. Ant. A Progreso km. 6, CORDEMEX, 97310, Mérida, Yucatán, México. \* E-mail: veleva@mda.cinvestav.mx, sauri\_ars16@hotmail.com  
† Electronic Supplementary Information (ESI) available: See  
DOI: 10.1039/x0xx00000x

evolution as a process crucial for the onset of instabilities, as a source of convection.

Li *et al.*<sup>18</sup> have suggested that electroreduction of  $\text{Fe}(\text{CN})_6^{3-}$  on a Pt electrode presents bistability coupled with convection feedback induced by hydrogen evolution, which accounts for the potential oscillations. The authors have elaborated a mechanism of galvanostatic potential oscillations, which should operate in the region of diffusion-limited current plateau.<sup>40-43</sup> As long as the current originating from a primary electrode process equals the imposed current, the electrode potential is stable. However, continuous depletion of the diffusion layer, caused by the electrode process and relatively slow diffusion, is the reason for a continuous decrease of a faradaic current, shifting the electrode to a more negative potential (for cathodic processes), at which the additional process, that is hydrogen evolution, takes place. The resulting detached bubbles of hydrogen cause the sudden convection, which replenishes the surface concentration of the primary reactant, and the current again rises above the diffusion-limited plateau, causing the return of the electrode potential to less negative values.

Galvanostatic potential oscillations have been also reported by Kaneko *et al.*<sup>19</sup> during electrodeposition of cadmium from alkaline cyanide electrolytes. When the electrolysis was carried out at current densities above the limiting one, hydrogen evolution occurs, acting as a source of convection. Vishomirskis<sup>44</sup> suggested that the reason for the galvanostatic potential oscillations is the formation/destruction of some passive film, formed on the surface of the electrode, and that hydrogen evolution does not play the main role originating the oscillations.

In our previous study, galvanostatic potential and potentiostatic current oscillations during the electrodeposition of cadmium from cyanide electrolytes on a Pt electrode were reported,<sup>21</sup> XPS investigations confirmed the existence of passive films at potentials corresponding to the onset of oscillations, which, besides the hydrogen evolutions under limiting current density, could be an additional promoter of the oscillatory behaviour of the system.

This study presents a detailed investigation of cathodic potential and current oscillations observed during the electrodeposition of cadmium from a cyanide electrolyte on a platinum electrode. Steady-state current-potential curves were recorded. The time series of the oscillations at galvanostatic and potentiostatic conditions were analyzed by the Fast Fourier Transform (FFT) and space phase projections. Electrochemical Impedance Spectroscopy (EIS), was used as an additional source of information to discuss the results. The goal of this study is to classify the oscillator behaviour.

## Experimental

Cadmium was deposited from a solution containing 0.14 M Cd as  $\text{CdSO}_4 \cdot 8/3 \text{H}_2\text{O} + 0.583 \text{ M KCN}$ . The electrolyte was prepared using chemicals of *pro analysis* purity and distilled water. The electrochemical experiments were performed in a

100  $\text{cm}^3$  three-electrode glass cell at room temperature. The vertical working electrode (area 1  $\text{cm}^2$ ), and the mesh counter electrode were made from platinum. A calomel reference electrode ( $E_{\text{Hg}/\text{Hg}_2\text{Cl}_2} = 0.2444 \text{ V vs SHE}$ ) was used. Preliminary preparation of the platinum working electrode includes pickling in a 50% solution of nitric acid, followed by polishing with 0.3 micron micropolish powder and cleaning with distilled water in a Branson ultrasonic cleaner equipment.

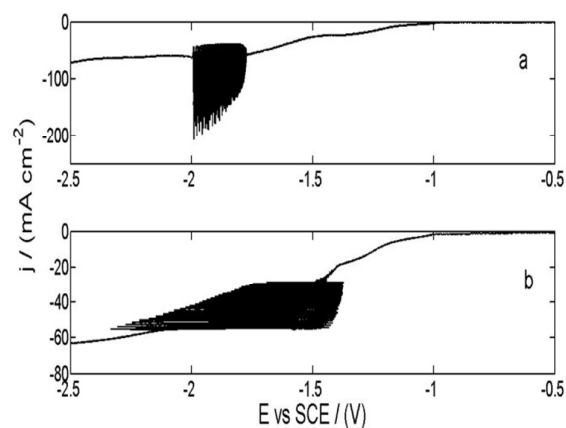
The current-potential curves, potentiostatic and galvanostatic time series experiments were carried out by means of a computerized potentiostat/galvanostat Series G 750 (Gamry Instruments Inc.) using the software PHE 200, and the Electrochemical Impedance Spectroscopy (EIS) from the software EIS 300. All potentials are referred to a saturated calomel electrode (SCE). The time series of the potentiostatic and galvanostatic curves were recorded with a sampling period of 0.001 s, and because of this, the time register was limited to 260 s. The selected sampling period was chosen because of the shape of the recorded curves depends on the number of obtained data.

## Results and discussion

### The voltammetric characteristics

The cathodic current-potential curves for Cd electrodeposition on a vertical platinum electrode, under potential (a) or current (b) scanning, are shown in Fig. 1.

The polarization curve obtained by potential sweep (Fig. 1(a)) shows a small current density plateau between -1.38 V and -1.47 V, which corresponds to the limiting current density for Cd electrodeposition ( $-22 \text{ mA cm}^{-2}$ ), where hydrogen production starts. At the potential of -1.75 V current oscillations appear accompanied by continuous hydrogen evolution from the surface of the electrode. However, current oscillations disappear at potentials more negative than -2.0 V, where intensive hydrogen evolution can be observed.



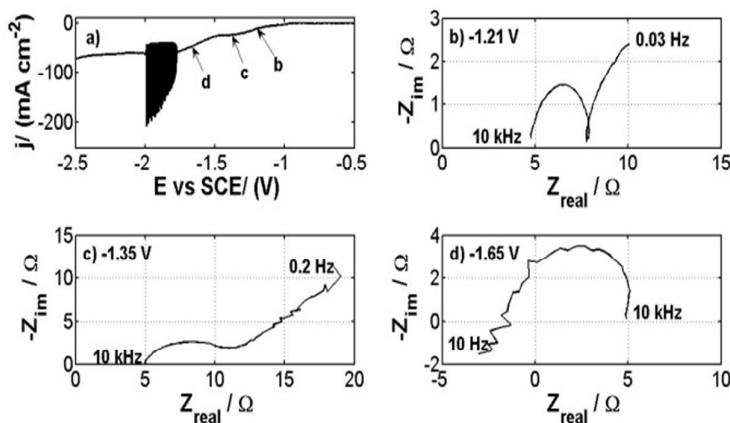
**Fig. 1** Cathodic polarization curves for deposition of Cd on a Pt electrode: (a) under potential sweep at  $10 \text{ mV s}^{-1}$ , and (b) under current sweep at  $0.1 \text{ mA cm}^{-2} \text{ s}^{-1}$ .

Figure 1(b) shows the cathodic polarization curve for Cd electrodeposition obtained by current scanning, when cathodic potential oscillations can be observed. The onset of the potential oscillations occurs at a current density of  $-22 \text{ mA cm}^{-2}$ , which corresponds to the limiting one. These potential oscillations are accompanied by pulsating hydrogen evolution. At current densities higher than  $-57 \text{ mA cm}^{-2}$ , the oscillations stop and intensive hydrogen evolution is observed. In both cases, the oscillations increase their amplitude, because of the imposed potential or current, respectively.

### Electrochemical impedance spectroscopy

Figure 2 presents the collection of impedance spectra recorded for Cd electrodeposition from a cyanide solution at potentials ( $-1.21 \text{ V}$ ,  $-1.35 \text{ V}$  and  $-1.65 \text{ V}$ ), chosen from the potentiodynamic current-potential curve (Fig. 2 (a)). In the first descending branch (positive slope in the polarization curve), only positive real impedance was observed in each potential value (Fig. 2 (b)), as well as in the range of the current density plateau (Fig. 2(c)). The electrochemical impedance spectrum presented in Fig. 2 (d) shows that the electrodeposition of Cd from a cyanide electrolyte has even more complex

characteristics. It can be seen (Fig. 2 (d)) that the impedance spectrum enters in the region of negative real impedance in a range of non-zero frequencies. This behaviour corresponds to the second descending branch of the current-potential curve (Fig. 2 (a)), where its slope is positive. This fact suggests the presence of a hidden negative resistance under dc conditions during Cd electrodeposition, belonging to Class IV (H-NDR oscillator), proposed in the classification for Strasser *et al.*<sup>39</sup> Because the attempts to measure the impedance spectra at frequencies lower than those indicated in Fig. 2 were unsuccessful, the EIS spectrum presented in Fig. 2 (d) does not reveal the whole shape expected for the H-NDR oscillator. It is expected that the loop beginning and ending must have positive real impedance, with the negative real impedance manifesting itself only for its intermediate regions. Based on the present results, it could be proposed that the electrodeposition of cadmium from a cyanide electrolyte on a vertical Pt electrode belongs to the HN-NDR type: an oscillator with a negative impedance spectrum in a region of positive slope in the N-Shape current-potential curve, which oscillatory behaviour is observed not only under potentiostatic conditions, but also under galvanostatic conditions (Fig. 1).



**Fig. 2** (a) Potentiodynamic current-potential curve for the electrodeposition of cadmium. (b-d) Impedance spectra at different potentials: (b)  $-1.21 \text{ V}$ , (c)  $-1.35 \text{ V}$  and (d)  $-1.65 \text{ V}$ .

### Potentiostatic current oscillations

Figure 3 shows the current oscillations observed during the electrodeposition of Cd. The onset of oscillations with small amplitude was registered at  $-1.7 \text{ V}$  (Fig. 3 (a)). At more positive potentials no current oscillations were observed. The amplitude of the oscillations increases with time, in the range between  $2 \text{ mA cm}^{-2}$  to  $10 \text{ mA cm}^{-2}$ . At a more negative potential,  $-1.8 \text{ V}$  (Fig. 3 (b)), an increase of the range in the oscillation amplitude ( $50 \text{ mA cm}^{-2}$  to  $100 \text{ mA cm}^{-2}$ ), is observed. Increasing the applied potential up to  $-1.9 \text{ V}$  (Fig. 3 (c)), the oscillation amplitude reaches the  $120 \text{ mA cm}^{-2}$ . At sufficient high potential (Fig. 3(d)), the current oscillations live for a short time. During potentiostatic electrodeposition, a

simultaneous continuous hydrogen evolution was observed from the cathode surface by naked eyes. At more negative potential, the hydrogen evolution is faster. The current oscillations can be observed for hours under appropriately controlled conditions.

It should be noted that even though there is continuous hydrogen evolution, the surface of the electrode is always covered by bubbles of hydrogen. The convection induced by the hydrogen evolution is always present causing a continuous replenishment of the Cd concentration. The changes on the electrode surface, due to the adsorbed hydrogen bubbles on said surface and their continuous evolution, or the formation of some passive layer,<sup>21</sup> could be the reason of the current oscillations.

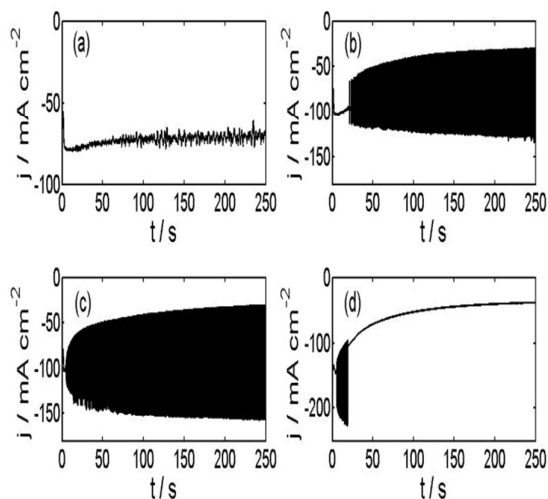


**Fig. 3** Time series at different voltage registered during the cathodic electrodeposition of cadmium: (a) -1.7 V; (b) -1.8 V; (c) -1.9 V, and (d) -2.1 V.

Figure 4 ((a)-(c)) presents a zoomed time scale of the behaviour of the first three time series (Fig. 3) and their respective Fast Fourier Transforms (Fig. 4 (d)-(f)). At the lowest potential (Fig. 4 (a)), only broadened peaks with high noisy background can be discerned (Fig. 4 (d)), which is characteristic of a chaotic behaviour. For periodic or quasi-periodic behaviour, a sharp fundamental frequency and a few harmonics can be clearly seen (Fig. 4 (e)-(f)). The frequency of the current oscillations diminishes with the increase of the applied potential.

Nonlinear analysis has been a useful tool for the study of instabilities in electrochemical systems.<sup>45-48</sup> The two-dimensional phase portraits, done with the delay method, for

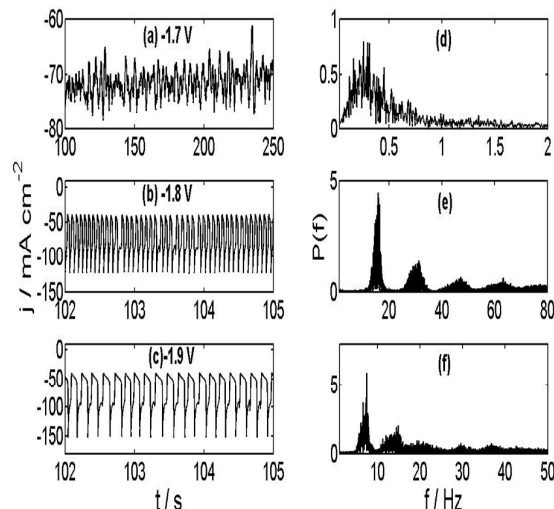


**Fig. 4** Zoomed time scale of the behaviour of the current oscillations during the electrodeposition of Cd for different potentiostatic conditions (a-b), and their corresponding Fast Fourier Transform spectra (d-f).

the time series obtained for electrodeposition of Cd at potentiostatic conditions, are presented in Fig. 5. A strange attractor can be seen (Fig. 5 (a)), which means chaotic behaviour. A torus attractor, characteristic for quasi-periodic behaviour, is shown in Fig. 5 (b), (d). Parts of the Fig. 5 (b), (d) are zoomed in Fig. 5 (c), (e), respectively, which show that two cycles of oscillations are present in the dynamical oscillatory behaviour. Those cycles, of small amplitude in the signal, correspond to those observed in Fig 4 (b), (c). The broadened band in Fig. 5 (b), (d), appeared because of a little variance in width and height of the oscillation peaks, due to the depletion of the reactants near the cathode during Cd electrodeposition.

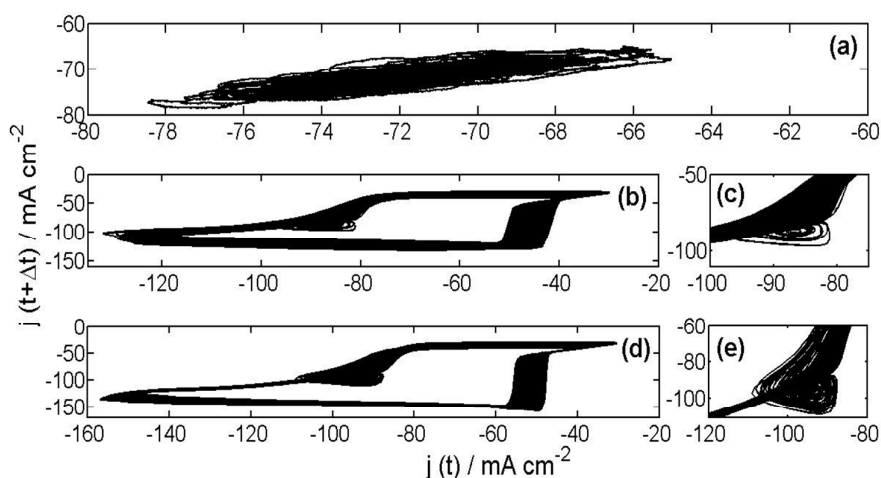


**Fig. 5** Two-dimensional phase portraits of the time series obtained for the electrodeposition of Cd at different potentials: (a) -1.7 V and  $\Delta t = 0.2$  s, (b) -1.8 V and  $\Delta t = 0.005$  s and (d) -1.9 V and  $\Delta t = 0.005$  s

### Gavanostatic potential oscillations

The time series of the cathodic potential oscillations registered during the electrodeposition of Cd on a vertical Pt electrode at different current densities are shown in Fig. 6. At current densities lower than  $-22 \text{ mA cm}^{-2}$  potential oscillations were not observed. Before the start of the oscillatory phase, different induction periods of several seconds are observed for the range of current densities between  $-22 \text{ mA cm}^{-2}$  and  $-60 \text{ mA cm}^{-2}$  (Figs. 6 (a)-(d)). At this point the potential falls to more negative values. It can be seen that the increase of the current density causes a reduction in the induction and oscillation periods, as a consequence of the higher rate (current density) of the Cd electrodeposition process and hydrogen production. During the potential oscillations pulsating simultaneous hydrogen evolution was observed. At the limiting current density ( $-22 \text{ mA cm}^{-2}$ , Fig. 6 (a)), the potential oscillations appear with an amplitude of about 400 mV, increasing in time up to 600 mV. At higher current densities the amplitude of the oscillations goes from 400 mV to 900 mV (Figs. 6 (b)-(c)).

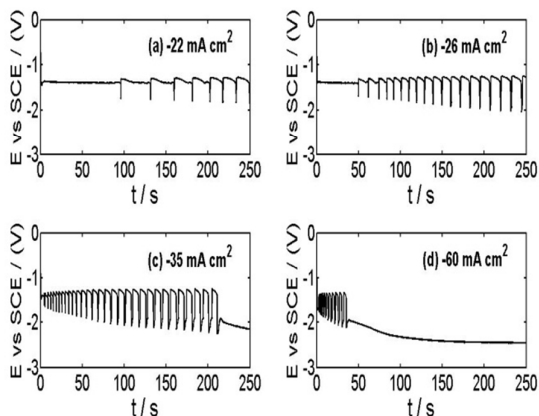


**Fig. 6** Time series at different current densities registered during the cathodic galvanostatic electrodeposition of cadmium: (a)  $-22 \text{ mA cm}^{-2}$ ; (b)  $-26 \text{ mA cm}^{-2}$ ; (c)  $-35 \text{ mA cm}^{-2}$ ; and (d)  $-60 \text{ mA cm}^{-2}$ .

At a higher current density, the potential oscillations live for a short time ( $-60 \text{ mA cm}^{-2}$ , Fig. 6 (d)), and they are no longer observable with the increase of current density. At this stage intensive hydrogen evolution occurs. The potential oscillations can be observed for a long time at the adequate conditions. The cathodic potential fluctuations are characterized by an abrupt shift to more negative values, when hydrogen bubbles detach from the surface of the electrode, and then return immediately to less negative (noble) potential. At this point the electrode surface starts to be covered by hydrogen bubbles, diminishing the active surface area, and as a consequence the potential again tends slowly to more negative values, followed by an abrupt shift to the most negative value, when the hydrogen bubbles detach, returning the cathodic potential to a less negative value.

Figures 7(a)-(c) present a zoomed time scale of the potential oscillatory behaviour during galvanostatic conditions (Fig. 6) and their respective Fast Fourier Transform (Fig. 7 (d)-(f)). It can be noted that the frequency increases when the applied current density is longer. However, the frequency diminishes in time.

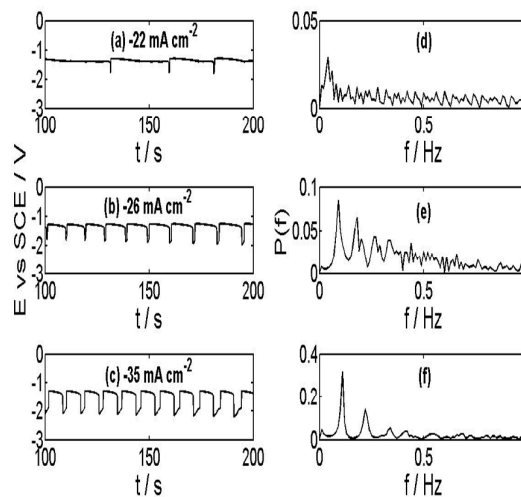


**Fig. 7** Zoomed time scale of the behaviour of the potential oscillations during the electrodeposition of Cd under different galvanostatic conditions (a-c), and their corresponding Fast Fourier Transform spectra (d-f).

The two-dimensional phase portraits, constructed with the delay method, for the time series of Cd electrodeposition at galvanostatic conditions, are presented in Fig. 8. At the studied conditions only torus attractors were observed, characteristic for quasi-periodic behaviour. The broadened band, similarly as in the case of potentiostatic current oscillations, appeared because of the variance in width and height of the oscillation peaks with time, due to the depletion of the reactants in the electrochemical solution.

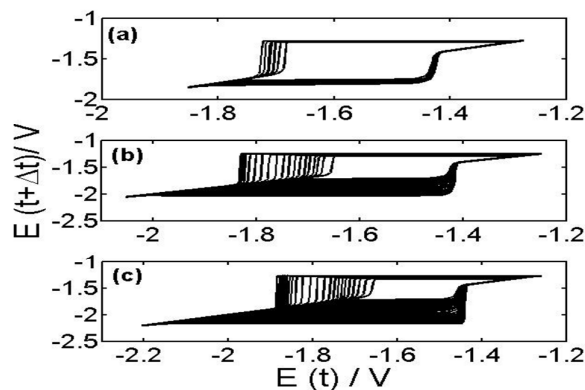


**Fig. 8** Two-dimensional phase portraits of the time series of Cd electrodeposition at different current densities: (a)  $-22 \text{ mA cm}^{-2}$  and  $\Delta t=0.005 \text{ s}$ , (b)  $-26 \text{ mA cm}^{-2}$  and  $\Delta t=0.01 \text{ s}$  and (c)  $-35 \text{ mA cm}^{-2}$  and  $\Delta t=0.01 \text{ s}$ .

## Conclusions

Cathodic current and potential oscillations were observed during electrodeposition of Cd from a cyanide electrolyte on a vertical Pt electrode, under potentiostatic and galvanostatic control, respectively.

The current-potential curve showed a typical (N-Shape) behaviour of electrochemical oscillators, in which a broad limiting current plateau exists. In the second descending branch with positive slope of the current-potential curve, the EIS experiments revealed a region of negative real impedance at high frequencies. This fact suggests the presence of a hidden negative differential resistance under dc conditions. The existence of current and potential oscillations, and the hidden negative differential resistance, allowed us to classify the cadmium electrodeposition process as an HN-NDR oscillator.

The observed oscillations could be mainly attributed to the changes on the real active cathodic area, due to the adsorption of the hydrogen molecule. The hydrogen ion reduction is a simultaneous process, which occurs always during the observed oscillations, replenishing the Cd ion concentration at the metal-electrolyte interface.

FFT revealed that the frequency of the current and potential oscillations increase at the higher potential and current density conditions, respectively.

The two dimensional phase portraits of the time series showed almost a quasi-periodic oscillation behaviour.

The complexity of the electrochemical behaviour makes the system an interesting subject for numerical simulations to obtain the mechanism of the oscillations, to reproduce the reported instabilities.

## Acknowledgements

This research was funded by a Doctor program grant of the Mexican Council of Science and Technology (CONACYT).

## References

- 1 G.T. Fechner, Schweigg., *J. Chem. Phys.*, 1828, **53**, 129.
- 2 M.T. Gorzkowski, A. Wesolowska, R. Jurczakowski, P. Ślepski, K. Darowicki and M. Orlik, *J. Solid State Electrochem.*, 2011, **15**, 2311.
- 3 M.T. Gorzkowski and M. Orlik, *J. Solid State Electrochem.*, 2011, **15**, 2321.
- 4 J. Wojtowicz, in *Modern Aspects of Electrochemistry*, ed. J. Bockris and B.E. Conway, Plenum Press, New York, 1973, vol. 9, p. 47.
- 5 U.F. Franck and R. FitzHugh, *Z. Elektrochem.*, 1961, **65**, 156.
- 6 J.J. Podesta, R.C.V. Piatti and A.J. Arvia, *J. Electrochem. Soc.*, 1979, **126**, 1363.
- 7 C.B. Diem and J.L. Hudson, *AIChE J.*, 1987, **33**, 218.
- 8 F. M. Schell and F.N. Albahadily, *J. Chem. Phys.*, 1989, **90**, 822.
- 10 M.R. Bassett and J.L. Hudson, *J. Phys. Chem.*, 1989, **93**, 2731.
- 11 O. Lev, A. Wolffberg, M. Sheintuch and L.M. Pismen, *Chem. Eng. Sci.*, 1988, **43**, 1339.
- 12 D. Sazou and M. Pagitsas, *J. Electrochem. Chem.*, 1992, **323**, 247.
- 13 M.C.H. McKubre and D.D. Macdonald, *J. Electrochem. Soc.*, 1981, **128**, 524.
- 14 M. Naito, H. Okamoto and N. Tanaka, *Phys. Chem. Chem. Phys.*, 2000, **2**, 1193.
- 15 G. Baier, U. Kummer and S. Sahle, *J. Phys. Chem. A*, 1999, **103**, 33.
- 16 J. Lee, P. Strasser, M. Eiswirth and G. Ertl, *Electrochim. Acta*, 2001, **47**, 501.
- 17 J. Lee, C. Eickes, M. Eiswirth and G. Ertl, *Electrochim. Acta*, 2002, **47**, 2297.
- 18 Z. Li, J. Cai and S. Zhou, *J. Electroanal. Chem.*, 1997, **432**, 111.
- 19 N. Kaneko, H. Nezu and N. Shinohara, *J. Electroanal. Chem.*, 1988, **252**, 371.
- 20 T. Tada, K. Fukami, S. Nakanishi, H. Yamasaki, S. Fukushima, T. Nagai, S.-I Sakai, Y. Nakato, *Electrochim. Acta*, 2005, **50**, 5050.
- 21 Ts. Dobrovolska, D.A. López-Sauri, L. Veleva and I. Krastev, *Electrochim. Acta*, 2012, **79**, 162.
- 22 S. Schaltin, K. Binnemans and J. Fransaer, *Phys. Chem. Chem. Phys.*, 2011, **13**, 15448.
- 23 F.W. Schlitter, G. Eickhorn and H. Fisher, *Electrochim. Acta*, 1968, **13**, 2063.
- 24 A. Survila and Z. Mockus, *Electrochim. Acta.*, 1999, **44**, 1707.
- 25 J.L. Hudson and T.T. Tsotsis, *Chem Eng. Sci.*, 1994, **49**, 1493.
- 26 K. Krischer, in *Modern Aspects of Electrochemistry*, ed. J. Bockris and B.E. Conway, Plenum Press, New York, 1999, vol. 32, p. 1.
- 27 M. Orlik, *Self-Organization in Electrochemical Systems*, ed. F. Scholz, Springer, Berlin Heidelberg, 2012, vol. 1.
- 28 M. Orlik, *Self-Organization in Electrochemical Systems*, ed. F. Scholz, Springer, Berlin Heidelberg, 2012, vol. 2.
- 29 M.T.M. Koper and J.H. Sluyters, *J. Electroanal. Chem.*, 1991, **303**, 65.
- 30 M.T.M. Koper and J.H. Sluyters, *J. Electroanal. Chem.*, 1991, **303**, 73.
- 31 M.T.M. Koper and J.H. Sluyters, *J. Electroanal. Chem.*, 1993, **352**, 51.
- 32 M.T.M. Koper and J.H. Sluyters, *J. Electroanal. Chem.*, 1993, **347**, 31.
- 33 M.T.M. Koper and J.H. Sluyters, *J. Electroanal. Chem.*, 1994, **371**, 149.
- 34 W. Wolf, M. Lübke, M.T.M. Koper, K. Krischer, M. Eiswirth and G. Ertl, *J. Electroanal. Chem.*, 1995, **399**, 185.
- 35 T.G.J. van Venrooij and M.T.M. Koper, *Electrochim. Acta.*, 1995, **40**, 1689.
- 36 M.T.M. Koper, *J. Chem. Soc., Faraday Trans.*, 1998, **94**(10), 1369.
- 37 P. Strasser, M. Lübke, C. Eickes and M. Eiswirth, *J. Electroanal. Chem.*, 1999, **462**, 19.
- 38 M.T.M. Koper, *J. Electroanal. Chem.*, 1996, **409**, 175
- 39 P. Strasser, M. Eiswirth and M.T.M. Koper, *J. Electroanal. Chem.*, 1999, **478**, 50.

- 40 Z. Li, J. Cai and S. Zhou, *J. Chem. Soc., Faraday Trans.*, 1997, **93**, 3519.
- 41 Z. Li, Y. Yu, H. Liao and S. Yao, *Chem. Lett.*, 2000, **4**, 330.
- 42 Z. Li, J. Cai, S. Zhou, *J. Electroanal. Chem.*, 1997, **436**, 195.
- 43 Z. L. Li, Q.H. Yuan, B. Ren, X.M. Xiao, Y. Zeng and Z.Q. Tian, *Electrochem. Commun*, 2001, **3**, 654.
- 44 R.M. Vishomirskis, *Kinetika Electroosazhdenia Metallov iz Kompleksnih Elektrolitov*, Nauka, Moskva, 1969.
- 45 M.T.M. Koper, P. Gaspard and J.H. Sluyters, *J. Chem. Phys.*, 1992, **97**, 8250.
- 46 M.T.M. Koper, P. Gaspard and J.H. Sluyters, *J. Phys. Chem.*, 1992, **96**, 5674.
- 47 S. Sadeghi and M. Thompson, *Phys. Chem. Chem. Phys.*, 2010, **12**, 6795.
- 48 D.A. López-Sauri, L. Veleza and G. Pérez, *Int. J. Electrochem. Sci.*, 2014, **9**, 1102.